I&EC research
Industrial & Engineering Chemistry Research
pubs.acs.org/IECR
Article

Separation of CO_2/N_2 onto Shaped MOF MIL-160(Al) Using the Pressure Swing Adsorption Process for Post-combustion Application

Mohsen Karimi,* Rafael M. Siqueira, Alírio E. Rodrigues, Farid Nouar, José A. C. Silva, Christian Serre, and Alexandre F. P. Ferreira

Cite This: *Ind. Eng. Chem. Res.* 2024, 63, 8772−8785
Read Online
ACCESS | Metrics & More | Article Recommendations | Supporting Information

ABSTRACT: Adsorption processes have already been considered as an appealing technology for carbon capture and climate change mitigation. Accordingly, this work investigated the capacity of shaped MIL-160(Al) as a water stable bioderived Al dicarboxylate microporous metal−organic framework for separation of carbon dioxide and nitrogen concerning postcombustion application. First, breakthrough experiments of carbon dioxide and nitrogen were accomplished at 313 K and 4.0 bar. Then, a set of equations/relations were considered to model the dynamic fixed-bed tests, in which the outcomes proved the capacity of the developed model for such a purpose. Next, a pressure swing adsorption (PSA) process with five steps, including pressurization, feed, rinse, blowdown, and purge, was planned and validated using performed experiments in a laboratory-scale PSA setup. In the end, an industrial PSA process was designed to attain a better grasp of the capacity of MIL-160(Al) for postcombustion application. The results indicated an exciting potential of this adsorbent for postcombustion carbon capture, with the purity and recovery of carbon dioxide around 67.3 and 99.1%, respectively.

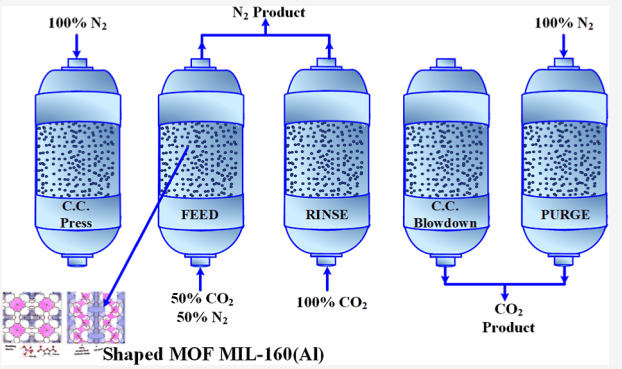

1. INTRODUCTION

1.1. Global Warming and Climate Changes. Carbon dioxide (CO_2) emissions related to anthropogenic activities have been linked to global warming and climate change.[1,2] The main CO_2 sources include the flue gas as a postcombustion source as well as biogas, natural gas, and syngas as precombustion processes.[3,4] Through the postcombustion sources, steel, cement, and petrochemical industries are considered the main ones.[2,5] According to the NASA report,[6−8] over the last century, global temperature has increased around 0.7 °C, which is almost 10 times faster than the average global warming since the Ice Age.[9,10] Furthermore, carbon dioxide emission has been enhanced with a rate of about 250 times faster in the mentioned period.[6,7] However, by the current rate, the concentration of carbon dioxide has a potential to reach around 570 ppm in the atmosphere by the end of the 21st century.[10,11] Accordingly, carbon capture and storage (CCS) is a vital approach in reducing carbon emissions and attaining the world net zero target.[12,13] Major attempts have been made to deploying highly efficacious technology (in terms of engineering prospects) or discovering novel sorbents (in terms of material science) for greenhouse gas (GHG) capturing.[14−16] In this way, different technologies have emerged for CO_2 capture and separation, in which chemical absorption, membrane, cryogenic distillation, and adsorption are among the most conventional ones,[17−19] A detailed description and comparison of these technologies can be found in the work by Karimi et al.[20] However, the adsorption technology using solid sorbents received a remarkable consideration based on its efficiency, operating continuously, and being eco-friendly,[21,22] while about efficient sorbents operate at different temperatures with proper service life and ease of regeneration requires more scrambles. More information concerning different configurations of adsorption-based reactors for CO_2 capture can be found in a study by Dhoke et al.[23]

1.2. Pressure Swing Adsorption. A successful pressure swing adsorption (PSA) design requires considering engineering aspects and material specifications simultaneously.[24] Regarding the process characteristics, flow rates, time and schedule of different steps, as well as pressure levels must be designed and optimized for developing a PSA process with a high yield.[25] On the other hand, the characteristics of employed materials as an adsorbent are the critical factor for developing favored PSA processes concerning the specific

Received: February 15, 2024
Revised: April 22, 2024
Accepted: April 25, 2024
Published: May 3, 2024

https://doi.org/10.1021/acs.iecr.4c00611
Ind. Eng. Chem. Res. 2024, 63, 8772−8785

applications. On these grounds, selectivity, adsorption capacity, stability, and ease of regeneration are some of the main specifications of appropriate adsorbent for separation processes.[25,26]

In this way, numerous efforts have been made to develop such an adsorbent, which resulted in different classes of materials, including zeolites,[27−29] activated carbons,[30,31] carbon molecular sieves,[25] and titanosilicates,[32] as well as more recently metal−organic frameworks (MOFs).[33,34] Among the mentioned sorbents, the MOFs as a category of crystalline hybrid micro- or meso-porous materials considering their appealing structural and textural properties have been nominated as a game-changer, which some of the recent interesting studies can found in different reports.[20,35,36] In this way, an integrated process was developed by Nikolaidis et al.,[37] as a two-stage P/VSA containing 13X and Mg-MOF-74 for CO_2 capture from postcombustion. Accordingly, the purity of CO_2 reached 40−60% in the first stage, while through the second stage, the purity reached 95%.[37] Furthermore, the capacity of HKUST-1 and MIL-101(Cr) for postcombustion application was investigated by Ye et al.[38] They reported that HKUST-1 is more promising for CO_2/N_2 separation comparing MIL-101(Cr) with CO_2 loading capacity of 1.82 and 1.17 mmol g^{-1}, respectively.[38] Also, the developed TSA demonstrated a better performance of HKUST-1 for CO_2 separation. In other study, Sabri et al.[39] investigated the amine-impregnated activated carbon—palm kernel shell (AC-PKS) for CO_2 capture from flue gas using a PSA process in a conceptual assessment. They reported that imidazole (IM) modification improves the working capacity as well as reduces the heat of adsorption. Also, simulated results showed that the purity of CO_2 is around 98%. The fundamental of the thermodynamic and kinetic of CO_2 capture using activated carbon was studied by Raganati et al.,[40] employing temperature swing adsorption cycles. The potential of zeolite 13X for postcombustion application was studied by Dantas et al.,[41] considering a five-step PSA process. They declared that the higher temperature of inlet flow (CO_2/N_2) demonstrates a positive impact on the purity of CO_2, which can be attributed to the high difference between the loading capacity of zeolite 13X for CO_2 and N_2. However, the highest purity reported for CO_2 was around 36.8%. A comparison between the capacity of activated and zeolite 13X for CO_2/N_2 separation was performed by Kacem et al.[42] It was found that zeolite 13X represents a higher purity for CO_2 separation than activated carbon. Hence, regarding aging over the cycles, zeolite 13X displayed a reduction on loading capacity followed by stabilization, while activated carbon demonstrated full reversible cycles. In other effort, zeolite 5A was studied for CO_2/N_2 separation employing a PTSA cycles which reported that a product with a purity higher than 95% is achievable for CO_2.[43] Also, based on accomplished simulation assessment for Mg-MOF-74 by Ben-Mansour et al.,[44] it was found that the PSA cycles with heat regeneration system might be beneficial due to reducing the number of cycles by getting the same separation performance. Furthermore, Pirngruber and Leinekugel-Le-Cocq[45] proposed a simple PSA approach to detect the target properties of a desire adsorbent concerning the mass transfer and equilibrium characteristics. In another study, Calgary framework-20 (CALF-20), as the recent benchmark of MOFs, was investigated for CO_2 and N_2 separation (15% CO_2:85% N_2) considering a light product pressurization. The outcomes indicated that 95% CO_2 purity and 90% recovery are achievable by CALF-20.[46]

1.3. Metal−Organic Frameworks. Routinely, MOFs are synthesized in various mechanisms accompanied by a wide range of tenability, porosity (pore size/shape), and functionalities (Bronsted of Lewis acid/basic sites, polar/apolar groups, etc.),[20,47] that contribute to developing sorbents with diverse domain in selectivity, kinetic, and thermodynamic.[35,36] In spite of the singular characteristics of MOFs, there are still some challenges in the way of development of these adsorbents, such as lack of chemical stability concerning the chemical agents, water vapor, or thermal shocks, as well as being in the powder form and the high synthesized cost.[32,34−36] However, other drawbacks are attributed to the amine-grafted MOFs, including amine loss all over the continuous operation, corrosion effect, and high energy consumption through the desorption step.[48] To overcome these constraints, recently, some of us introduced the bioderived Al-based MOF MIL-160 as a robust microporous adsorbent in the shaped form which has been synthesized from the bioderived 2,5 FDCA (FDCA stands for furane dicarboxylic acid) ligand.[49,50] This sorbent also represents acceptable characteristics for the heat pump/chiller applications.[50−52] Besides that, this material can be produced under green ambient pressure conditions and shaped easily using wet granulation,[53] with production at an industrial scale.[54] Of note, a techno-economic synthesis evaluation of MIL-160(Al) demonstrated admissible cost values upon industrial-scale production.[55] Additionally, fundamental adsorption properties of this 1D channel microporous solid, including adsorption capacity, selectivity, heat of adsorption, and kinetic assessment, have already proved the acceptable potential of MIL-160(Al) for CO_2 and N_2 separation for postcombustion application.[49,56]

1.4. Research Objective. In this work, the potential of MIL-160(Al) as a water stable and shaped form MOF for CO_2/N_2 separation using the PSA process has been studied for the first time. To this purpose, first, the fixed-bed adsorption of CO_2 and N_2 has experimentally been performed and simulated by gPROMS. The breakthrough assessments were accomplished at 318 K and 4.0 bar, to have some precise knowledge about the dynamic of system and get a reliable approach for designing the cyclic adsorption process. Afterward, regarding the dynamic simulation outcomes, a PSA process was designed and experimentally validated by a laboratory-scale PSA setup. Indeed, the laboratory-scale PSA process was performed at 318 K and 4.5 bar, which in this case was planned to validate the design PSA process concerning the potential of MIL-160(Al) for separation of CO_2/N_2. Truly, there are a good agreement between experimental and simulation results in both dynamic assessment and developed cyclic process. Finally, to better understand the capacity of MIL-160(Al) for large-scale application related to the postcombustion process, an industrial VPSA process has been designed/investigated, for CO_2 capturing from flue gas stream containing CO_2/N_2 (15%:85%) at 318 K and 4.5 bar. It is worth noting that based on the different point-sources of CO_2 emission, there may be some differences on the temperature and pressure.

2. MATERIALS AND METHODS

2.1. Materials. The synthesis protocol and the main specifications of shaped MIL-160(Al) were reported in a study by Cadiau et al.,[51] and Permyakova et al.,[50] also, the textural properties, the main characterization, and N_2 adsorption−

https://doi.org/10.1021/acs.iecr.4c00611
Ind. Eng. Chem. Res. 2024, 63, 8772−8785

desorption at 77 K can be found in a study by Karimi et al.[49] However, some of the main properties are represented in Table 1.[49] Furthermore, the different gases, such as carbon dioxide (99.99%), nitrogen (99.95%), and helium (99.999%), were provided by L'Air Liquide.

Table 1. Summary of Textural Properties of Shaped Form Al-Based MOF MIL-160[49]

adsorbent properties	
parameter	numerical values
particle radius (m)	0.001
bulk density at 0.0037 MPa (g/mL)	1.07
apparent (skeletal) density at 206.5 MPa (g/mL)	1.40
median pore diameter (volume) at 7.7 MPa and 0.1 mL/g (μm)	0.162
median pore diameter (area) at 119.8 MPa and 9.7 m^2/g (μm)	0.0104
average pore diameter (4 V/A) (μm)	0.0454
total intrusion volume at 206.5 MPa (mL/g)	0.22
total pore area at 206.5 MPa (m^2/g)	19.45
micropore volume (cm^3/g)	0.336

2.2. Experimental Setup. In this work, the dynamic adsorption experiments as well as laboratory-scale cyclic adsorption tests were accomplished in an existing setup. The temperature was continuously recorded in the apparatus by using a thermocouple placed at the middle of the column. The compositions at the outlet flow were also continuously monitored by an infrared gas analyzer. The flow rates at the inlet were controlled using mass flow controllers, and also the flow rate at the outlet flow was monitored using a mass flow meter. In addition, the pressure in the system was controlled by using a backpressure regulator. A simple view of this apparatus is illustrated in Figure 1, and more details can be found elsewhere.[33] The main characteristics of the considered setup, accompanied by operating conditions, are reported in Table 2.

Table 2. Characteristics and Considered Operating Conditions of Experimental Setup to Accomplish the Breakthrough and PSA Experiments

operating conditions	numerical values
F (flow rate) (mL/min)	200
T (temperature) (K)	318
P (pressure) (bar)	4
adsorbent properties	
parameter	numerical values
bed porosity (m^3_{void}/m^3_{bed})	0.48
particle porosity (m^3_{void}/m^3_{bead})	0.31
mass of sample (raw) (g)	12.2
mass of sample (activated) (g)	10.9
adsorbent properties	
bed characters	numerical values
bed length (cm)	6.8
bed diameter (cm)	2.1
bulk solid density of adsorbent (kg/m^3)	463.03

2.3. Experimental Procedure. To accomplish the dynamic experiments (breakthrough and cycles), the sample, shaped MIL-160(Al), was first activated by passing the helium in the column with the flow rate of 327.5 NmL/min, a heating

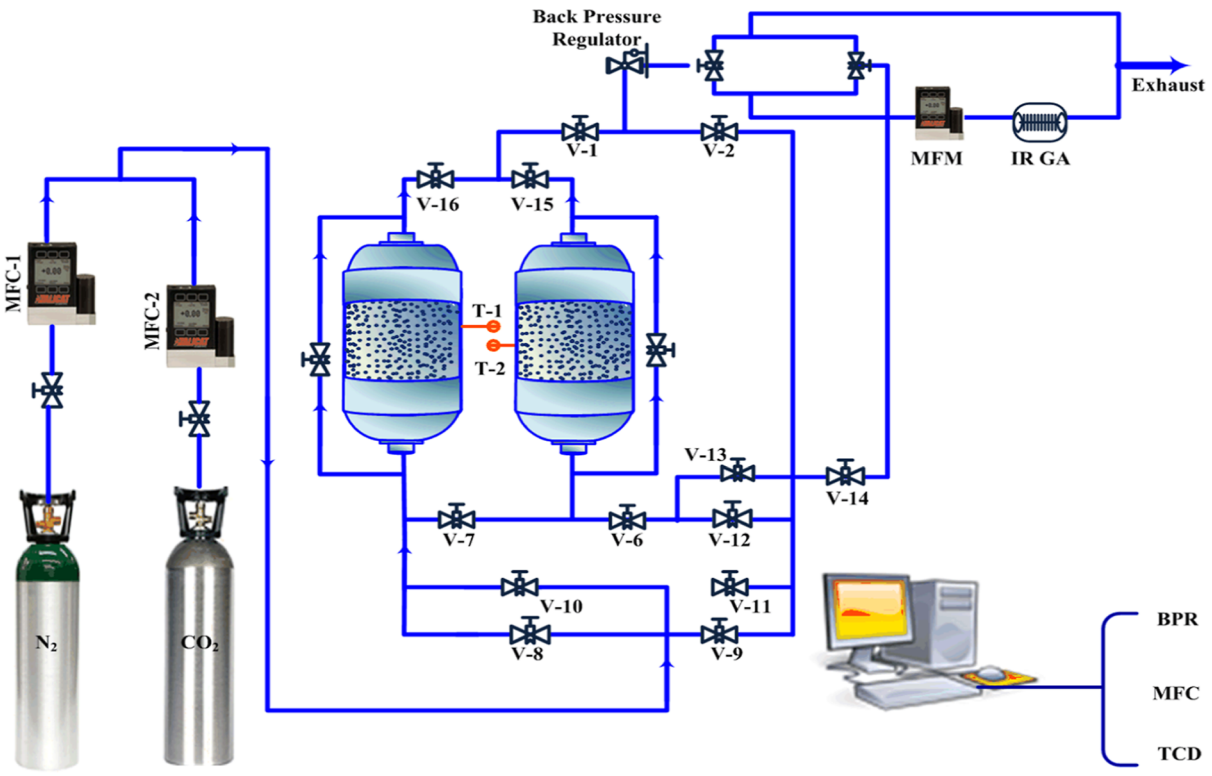

Figure 1. Simple schema of the experimental setup to accomplish breakthrough and PSA experiments.

https://doi.org/10.1021/acs.iecr.4c00611
Ind. Eng. Chem. Res. 2024, 63, 8772−8785

Table 3. Detailed Descriptions of Different Steps of the Laboratory-Scale Designed PSA Process for CO_2/N_2 Separation Using Shaped MIL-160(Al)

PSA steps	PSA variables					
	temperature (K)	pressure (bar)	flow rate (mL/min)	step time (s)	CO_2 (%)	N_2 (%)
pressurization	318	1 → 4.5	800	65		100
feed	318	4.5	600	350	50	50
rinse	318	4.5	200	160	100	0
blowdown		4.5 → 1.0		240		
purge		1.0	75	240		100

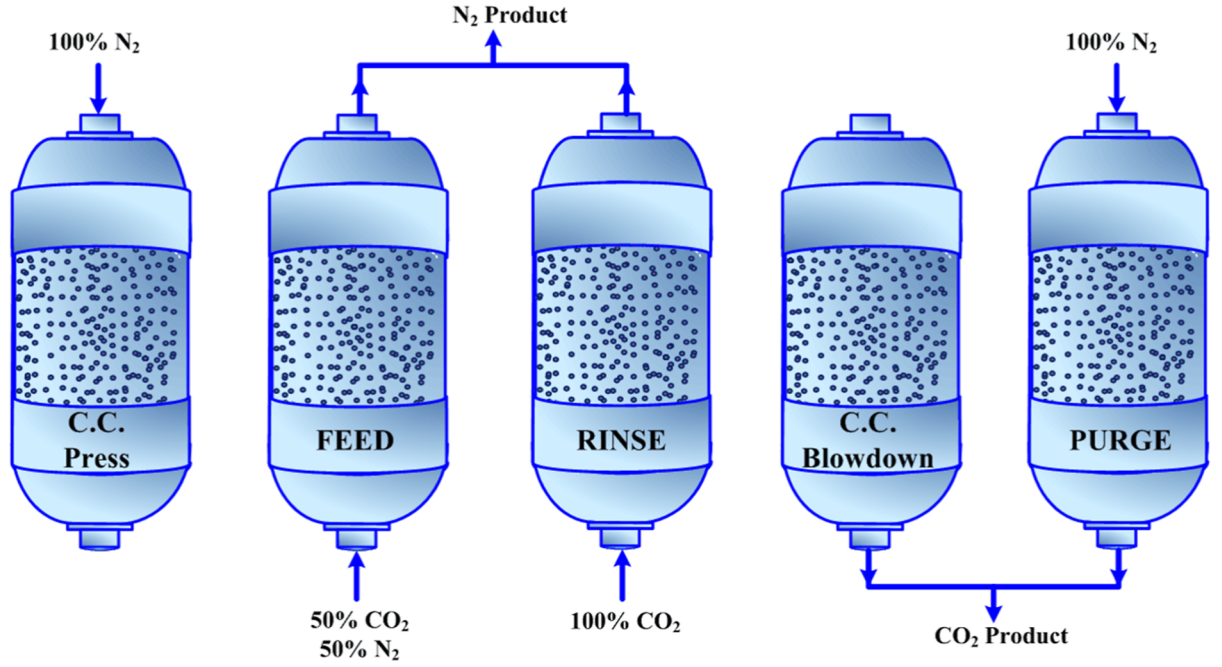

Figure 2. Considered five different steps in the designed PSA process for separation of the CO_2/N_2 mixture.

rate of 1 K/min, up to 423 K, overnight. In this way, to acquire the dynamic behavior of adsorption of the considered adsorbent, the fixed-bed breakthrough tests were experimentally accomplished at 4 bar and 318 K. Accordingly, the column was initially saturated with nitrogen; then a flow containing CO_2 (50%)/N_2 (50%) was fed to the bed, while the process was fulfilled using pure flow of carbon dioxide. In the next experiment, the bed was first saturated with nitrogen; afterward, a pure flow of carbon dioxide was fed to the adsorption column until a saturated/equilibrium condition. Next, the desorption of carbon dioxide was performed by using a pure flow of nitrogen. The pressure, temperature, and composition of the fixed-bed column were continuously monitored and recorded.

Additionally, the cyclic experiments were carried out by saturating the column with N_2, and afterward the gas mixture CO_2/N_2 was fed to the system. The experimental cyclic experiment was performed in five different steps at 318 K and 1−4.5 bar. Accordingly, the first step (counter-current pressurization) was performed with N_2, then the adsorption step performed, followed by the rinse with the pure CO_2. Afterward, the blowdown and purge steps were accomplished. A detailed description of the different steps of the developed cyclic pressure tests is reported in Table 3. The experimental five different steps have been schematically illustrated in Figure 2. It is worth noting that because of the restrictions of available experimental setup, the cyclic adsorption experiment was performed with 50% of carbon dioxide. Yet, the industrial PSA process has been designed and evaluated for a feed with CO_2 (15%)/N_2 (85%) composition.

3. MATHEMATICAL MODEL

Developing a PSA process requires a robust support concerning the adsorption equilibrium values and accurate simulation approaches. To this end, first, the equilibrium data shall be represented by a proper model. To date, several empirical and theoretical models were developed (a summary of the main ones can be found in a study by Foo & Hameed[57]), in which the Langmuir model,[58] regarding its simplicity and user-friendliness is among the most interesting ones for designing the cyclic adsorption processes.[59,60] The basic fundamentals and assumptions of this approach are as follows: (i) adsorption occurs only on a finite number of sites which are definite,[61] (ii) there are no lateral interaction among adsorbed molecules,[62] (iii) all sites possess the same adsorption energy,[63] and (iv) for the mixed gas Langmuir, the saturation capacities of all components are required to be the same to be thermodynamically consistent.[64] Hence, in the current study, this model was considered for the evaluation of adsorption equilibrium outcomes and designing the PSA cycles; this model has been described in Appendix A (Supporting Information).

After the adsorption equilibrium results are obtained, the dynamic fixed-bed adsorption breakthrough results are

https://doi.org/10.1021/acs.iecr.4c00611
Ind. Eng. Chem. Res. 2024, 63, 8772−8785

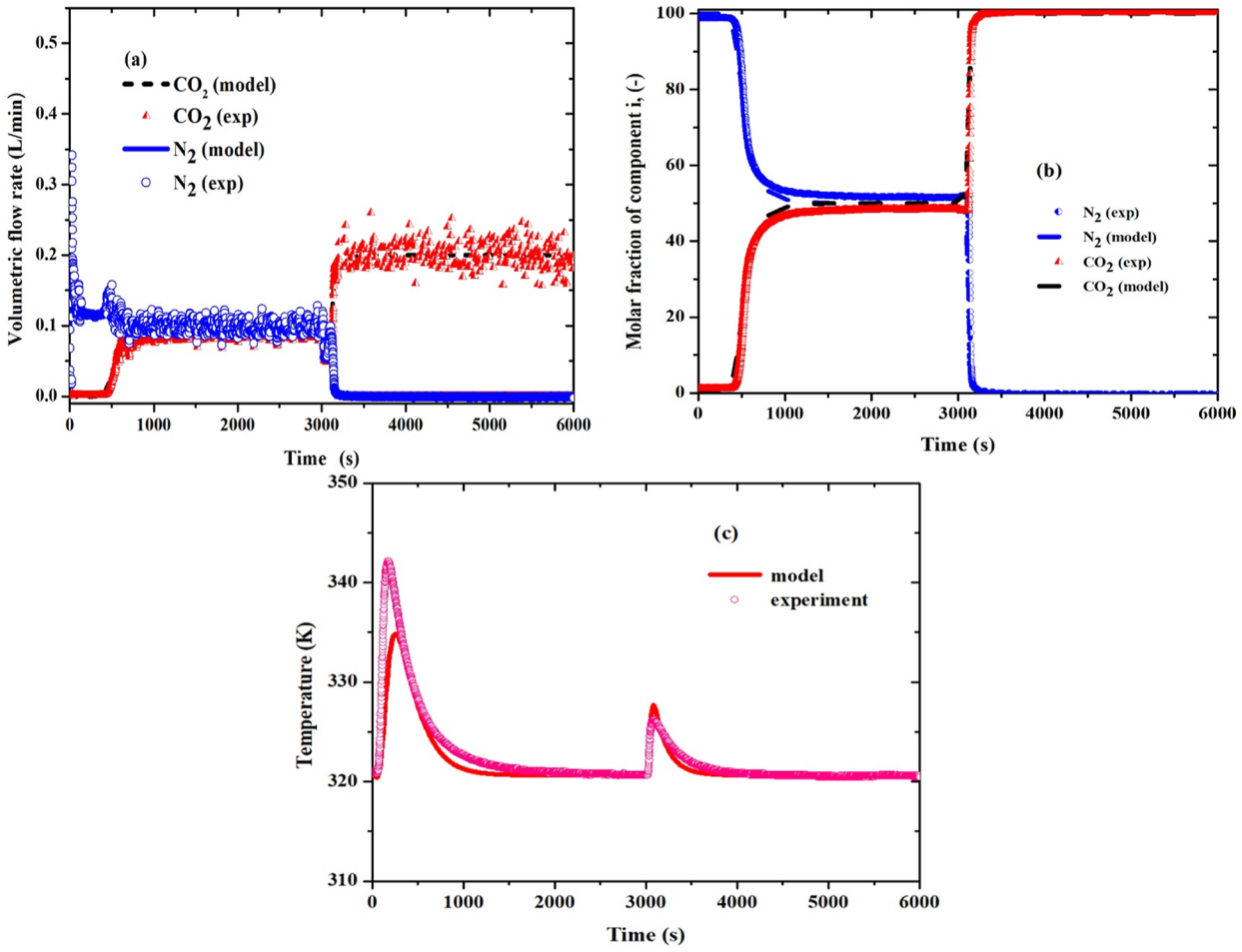

Figure 3. Breakthrough experiment and simulation result of carbon dioxide and nitrogen over the bed initially saturated with nitrogen, the desorption with pure carbon dioxide, and experiment at 318 K and 4.0 bar. (a) Flow rates, (b) molar fraction, and (c) temperature history. Symbols represent experimental results, and lines indicate model outcomes.

modeled using a set of governing equations, including mass, energy, and momentum balances. In addition, some auxiliary relations and empirical correlations are required to estimate the mass and heat transport parameters. Then, some assumptions are considered for the mathematical modeling of the adsorption process, including (i) gas phase described by the ideal gas law, (ii) mass transfer considered as a lumped overall resistance, (iii) axial dispersion assumed in the column, (iv) energy balance qualified as a nonisothermal model, and (v) pressure drop calculated with the Ergun equation.[65−67] In the next step, the PSA cycles are designed using the simulation outcomes of fixed-bed experiments. To this end, regarding the CO_2 capture purpose of the study, some appropriate boundary conditions are required, which are reported in Table S1 (Supporting Information). A summary of employed mathematical modeling equations and auxiliary relations is reported in Appendix A.

On the other hand, routinely, cyclic adsorption processes (PSA, TSA, VPSA, etc.) are evaluated concerning the purity, recovery, productivity, and energy consumption, which are defined by 16[68]

$$N_2\ \text{purity}\ (\%) = \frac{\sum_j \left(\int_0^{t_j} F_{N_2,\text{out}}\, dt \right)}{\sum_j \left(\int_0^{t_j} F_{N_2,\text{out}}\, dt + \int_0^{t_j} F_{CO_2,\text{out}}\, dt \right)} \times 100 \quad (1)$$

$$N_2\ \text{rec}\ (\%) = \frac{\sum_j \left(\int_0^{t_j} F_{N_2,\text{out}}\, dt \right) - \sum_k \left(\int_0^{t_k} F_{N_2,\text{in}}\, dt \right)}{\sum_l \left(\int_0^{t_j} F_{N_2,\text{in}}\, dt \right)} \times 100 \quad (2)$$

$$CO_2\ \text{purity}\ (\%) = \frac{\sum_m \left(\int_0^{t_m} F_{CO_2,\text{out}}\, dt \right)}{\sum_m \left(\int_0^{t_m} F_{CH_4,\text{out}}\, dt + \int_0^{t_m} F_{CO_2,\text{out}}\, dt \right)} \times 100 \quad (3)$$

$$CO_2\ \text{rec}\ (\%) = \frac{\sum_m \left(\int_0^{t_m} F_{CO_2,\text{out}}\, dt \right) - \sum_m \left(\int_0^{t} F_{CO_2,\text{in}}\, dt \right)}{\sum_l \left(\int_0^{t_l} F_{CO_2,\text{in}}\, dt \right)} \times 100 \quad (4)$$

$$\text{Productivity}\ (\text{mol kg}^{-1}\,\text{h}^{-1}) = \frac{\sum_j \left(\int_0^{t_j} F_{CO_2,\text{out}}\, dt \right) - \sum_k \left(\int_0^{t_k} F_{CO_2,\text{in}}\, dt \right)}{\text{mass of dry adsorbent} \times t_{\text{cycle}}} \quad (5)$$

where l is the feed, counter-current pressurization, j is the feed, rinse, k is the purge, countercurrent pressurization, and m is

https://doi.org/10.1021/acs.iecr.4c00611
Ind. Eng. Chem. Res. 2024, 63, 8772−8785

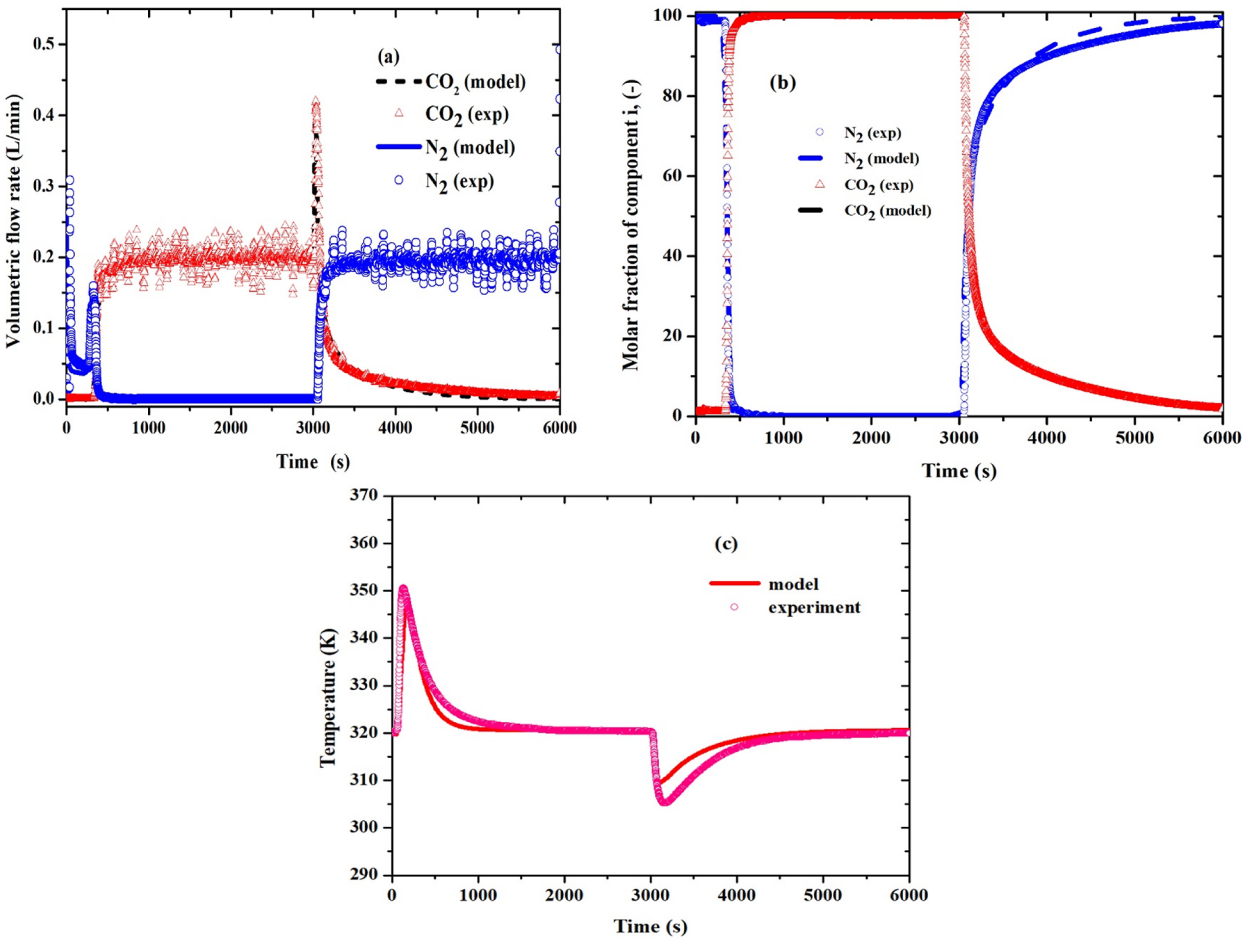

Figure 4. Carbon dioxide adsorption over a fixed bed column initially saturated with nitrogen and desorption accomplishes also with pure nitrogen, experiment at 318 K and 4.0 bar. (a) Flow rates, (b) molar fraction, and (c) temperature history. Symbols represent experimental results, and lines indicate model outcomes.

the blowdown and purge. Additionally, the energy consumption was calculated by[69]

$$\text{Energy consumption} = \frac{1}{\eta}\dot{n}R_g T_g \frac{\gamma}{\gamma - 1}\left(\left(\frac{P_H}{P_L}\right)^{\gamma-1/\gamma} - 1\right) \quad (6)$$

where $\dot{n}$ is the molar flow rate, R_g is the ideal gas constant, T_g is the gas temperature, η is the pump efficiency (assumed η = 80% for compressor and η = 60% for vacuum pump), and γ is the specific heat ratio of the gas ($\gamma = \frac{C_P}{C_V}$), as well P_L and P_H indicate the lower and higher pressure, respectively. Finally, the developed system of algebraic-differential equations was solved by the gPROMS considering a second-order orthogonal collocation over 28 finite elements.

4. RESULTS AND DISCUSSION

4.1. Breakthrough Experiments and Simulation. Routinely, the transient response of the adsorption column to a specific change in the feed mixture is basic information to assess the capacity of sorbent for desired separation applications. On these grounds, the accordance of experimental results and simulation values of dynamic breakthrough measurements validates the developed model to be employed for designing the cyclic adsorption process. To this end, in the first step, the dynamic breakthrough experiments onto shaped MIL-160(Al) were experimentally performed and numerically simulated at a temperature of 318 K and total pressure of 4 bar. Afterward, a PSA process was designed for CO_2/N_2 separation as high as purity and recovery possible. Figure 3 illustrates carbon dioxide and nitrogen adsorption onto shaped MIL-160(Al) (3a flow rate, 3b, molar fraction, and 3c temperature history), in which the bed was initially saturated with pure nitrogen. Although in Figure 4 experiment, the bed was initially saturated with N_2; thereafter, a pure flow of CO_2 was introduced to the system until saturation, and then the subsequent CO_2 desorption was accomplished using a pure N_2 flow. As shown in Figures 3 and 4, there is an acceptable agreement between the experimental results and simulation outcomes of dynamic adsorption experiments, which proves that the developed model predicts well the dynamic adsorption of CO_2 and N_2 onto shaped MIL-160(Al).

Regarding the temperature histories in Figures 3 and 4 which resulted from a nonisothermal and nonadiabatic column operation, it can be observed at the beginning of adsorption processes that there are peaks in the temperature history. It is worth noting that through the first breakthrough experiment (Figure 3), the temperature increment presented a lower value than the second one from Figure 4, in which only pure CO_2 is adsorbed. It can be explained due to the fact that only half the amount of CO_2 was fed in the first experiment (50/50%

https://doi.org/10.1021/acs.iecr.4c00611
Ind. Eng. Chem. Res. 2024, 63, 8772−8785

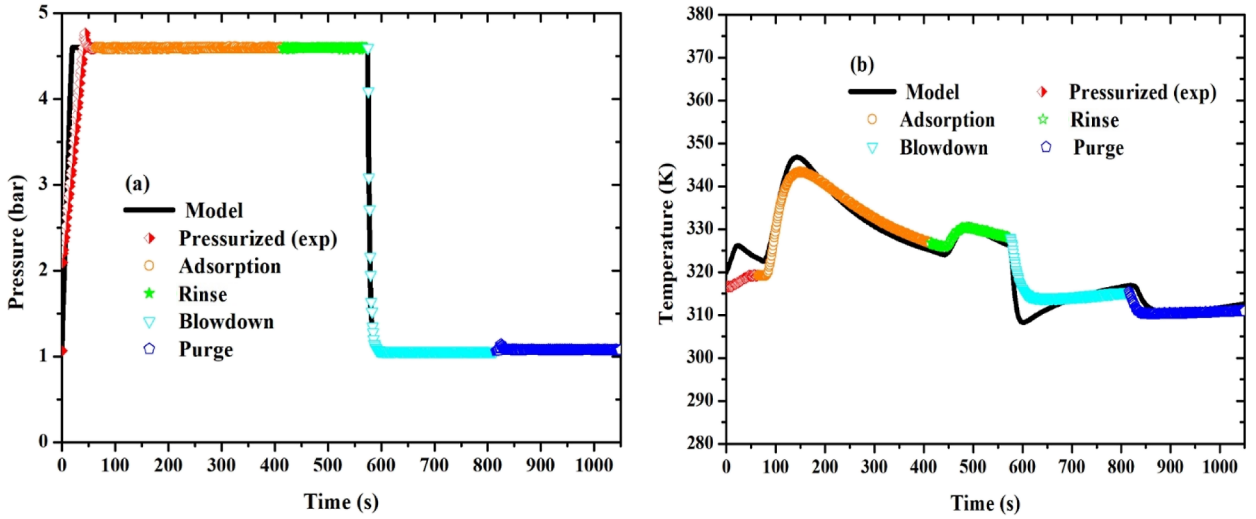

Figure 5. (a) Pressure and (b) temperature history of the designed laboratory-scale PSA process (cycle no. 8 as a cyclic steady state) for separation of CO_2/N_2 at 318 K and 4.5 bar. Symbols illustrate experimental outcomes, and lines specify modeling results.

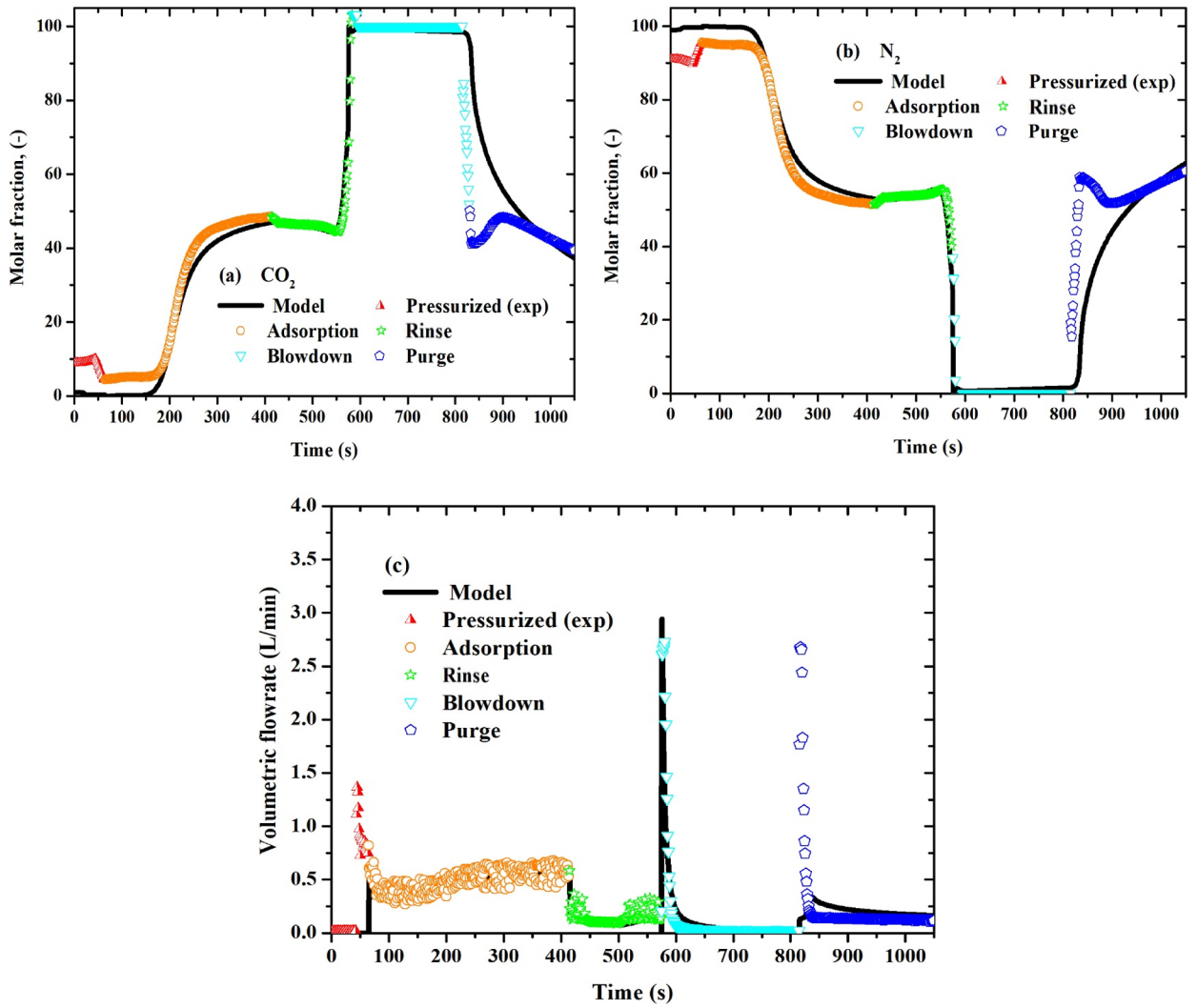

Figure 6. (a) Molar fraction of carbon dioxide, (b) molar fraction of nitrogen, and (c) total flow rate of designed laboratory-scale PSA process (cycle no. 8 as a cyclic steady state) for separation of CO_2/N_2 at 318 K and 4.5 bar. Symbols illustrate experimental outcomes, and lines specify modeling results.

https://doi.org/10.1021/acs.iecr.4c00611
Ind. Eng. Chem. Res. 2024, 63, 8772−8785

mixture) comparing to the second one (100% CO_2). Since the CO_2 adsorption heat is higher than the N_2 one (see Table S3), the amount of CO_2 then has a great influence on the history of temperature. Hence, in Figure 4, a reverse behavior is observed during the CO_2 desorption step. During the respective step of the experiment, the complete CO_2 desorption was performed, and although N_2 was being adsorbed, the temperature even decreased. Nonetheless, these behaviors can be attributed to the exothermic and endothermic nature of adsorption and desorption processes, respectively. Accordingly, by initiating the sorbates adsorption in the column, a significant amount of heat is released, in which after a while the equilibrium temperature is acquired, as well as the corresponding reverse is expected in the CO_2 desorption step (Figure 4).

It should also be mentioned that the numerical simulation was developed by considering the axial dispersion effect in the fixed-bed column by employing Langer et al. correlation (E.S.12, Appendix A).[59,60] Other considered auxiliary relations/correlations are completely discussed in Appendix A. Accordingly, concerning the promising experimental and simulation results of dynamic fixed-bed outcomes, a PSA unit was designed for CO_2 and N_2 separation.

4.2. Laboratory-Scale Cyclic Adsorption Experiment. After a robust modeling topology was established for the dynamic fixed-bed adsorption of CO_2 and N_2, a cyclic experiment was planned to have a precise assessment of the potential of MIL-160(Al) concerning CO_2/N_2 separation. In this way, five steps were considered: (i) pressurization with pure N_2 in a counter-current way, (ii) feed (adsorption), (iii) rinse with CO_2, (iv) blow down, and (v) purge with counter-current N_2. It is worth noting that the first step was controlled by defining the total pressure of the column at 4.5 bar, while other ones were controlled regarding the time. Accordingly, the adjusted time of different steps includes feed step-350 s, rinse step-160 s, blowdown step-240 s, and purge step-240 s. It should also be considered that the cyclic steady state (CSS) was obtained after around five cycles. More specifications related to each step are illustrated in Table 3.

The experimental and simulation outcomes for a CSS are illustrated in Figures 5 and 6, as well as the full experimental cycles have been represented in Figure S2. As shown in Figure 5a, the pressure through the pressurization step increased to reach the set point; afterward, the adsorption with a flow of CO_2/N_2 (50%:50%) and rinse steps is followed at the same pressure (4.5 bar). Next, the regeneration/desorption of saturated bed is accomplished using blowdown and purge, in which during these steps the pressure is dropped until atmospheric pressure. Regarding the temperature history presented in Figure 5b, as can be found, a temperature variation around 25 K is observed, which is ascribed to the nature of the process. Figure 6 displays the dominant tendency of nitrogen and carbon dioxide during the designed process. As displayed in Figure 6b, the column has first been pressurized with pure nitrogen and getting ready for the feed step. However, the adsorption step for separation of carbon dioxide and nitrogen was tested with 50−50% feed. To enhance N_2 recovery and CO_2 purity, the CO_2 concentration is increased through the rinse step. As a subsequence of blowdown, the countercurrent purge step is fulfilled with pure N_2 flow to regenerate the bed properly. Totally, as can be observed in Figures 5 and 6, the developed model predicts well the dynamic of the process and proves its promising capacity.

4.3. Industrial Scale PSA Evaluation. In the last effort, to have a better knowledge on the potential of MIL-160(Al) for postcombustion application in the large scale, an industrial PSA has been designed to treat a flue gas stream containing CO_2/N_2 (15%:85%). Accordingly, the specifications and characterizations of industrial plant were required, which were considered based on the reported values of Ferreira et al.[33] and Agarwal et al.[70] The industrial PSA process was designed with five steps: pressurization, feed, rinse, blowdown, and purge. The detailed descriptions of bed, specifications, and performance of process are reported in Table 4. Also, a simple schema of different steps of the designed process is illustrated in Figure 7. It is worth noting that in this case study, the feed was pressurized until 4 bar, while through the blowdown and purge steps, the bed was regenerated with vacuum around 0.2 bar. The bed was also modeled in a nonadiabatic and nonisothermal operation. Accordingly, each cycle of this VPSA process lasts around 880 s, which contains 200 s for pressurization, 200 s for feed step, 120 s for rinse step, as well as 160 s for blowdown and 200 s to accomplish the purge.

Table 4. Characteristics, Specifications, and Performance of the Designed Industrial VPSA Process for CO_2 Capturing from Flue Gas Using Shaped MIL-160(Al)

bed specifications				
	bed length (m)	bed diameter (m)	bed volume (m^3)	bed area (m^2)
value	5	1.5	10.61	1.77
bed characteristics				
	bed density (kg/m^3)	particle radius (m)	bed porosity (−)	
value	532.45	1.35×10^{-3}	0.487	
PSA steps	PSA variables			
	temperature (K)	pressure (bar)	flow rate (L/min)	step time (s)
pressurization	318	1 → 4.5	21,000	200
feed	318	4.5	100,000	200
rinse	318	4.5	30,000	120
blowdown		4.5 → 0.2	0	160
purge		0.2	6000	200
performance of designed industrial PSA				
	purity (%)	recovery (%)	productivity(mol kg^{-1} h^{-1})	
N_2	99.3	81.1	24.43	
CO_2	67.31	99.1	3.046	

The industrial VPSA was simulated during 50 cycles, the CSS is represented in Figures 8 and 9, also the last CSS cycles have been displayed in Figure S3 (Supporting Information). It should be noted that after around 17 cycles, the CSS was achieved. The pressure variations through the cycle have been specified in Figure 8a, as well the temperature history have been illustrated in Figure 8b. As can be seen in Figure 8a, during the pressurization step, the pressure is increased until 4.5 bar, which contributes to a temperature increment within the bed, as shown in Figure 8b. Then, the feed and rinse steps were followed at constant pressure (4.5 bar), and in these steps because of CO_2 adsorption, a temperature enhancement was expected, as observed in Figure 8b. Finally, a remarkable reduction in both temperature and pressure occurs through the blowdown and purge as regeneration/desorption steps.

The molar fractions of carbon dioxide and nitrogen as well as the profile of flow rate through the CSS are presented in

https://doi.org/10.1021/acs.iecr.4c00611
Ind. Eng. Chem. Res. 2024, 63, 8772−8785

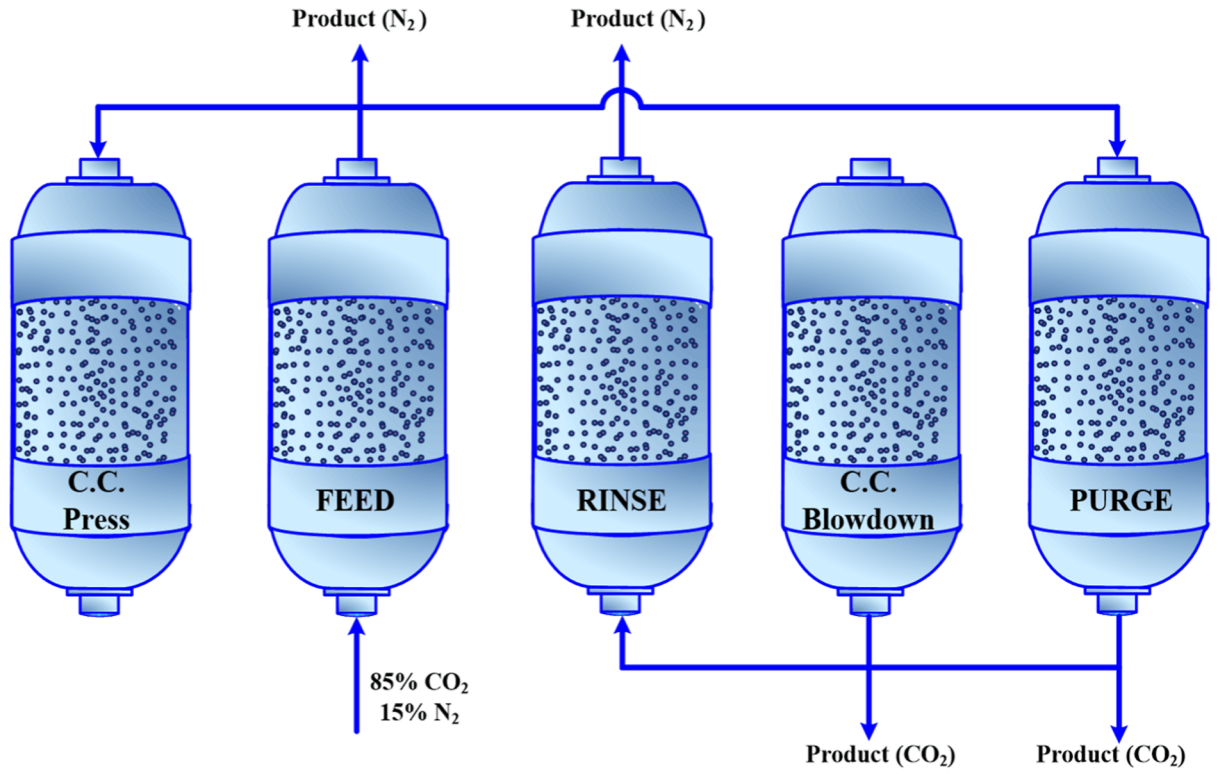

Figure 7. Simple schema of different steps of the designed industrial VPSA process for CO_2 capturing from flue gas.

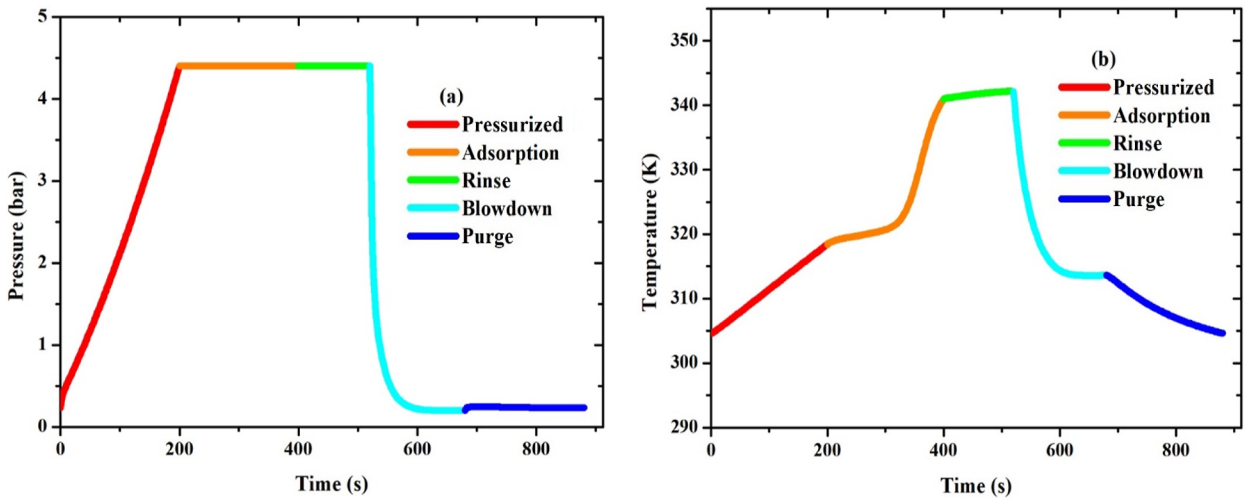

Figure 8. (a) Pressure and (b) temperature history of the designed industrial VPSA process for CO_2 capture from flue gas using shaped MIL-160(Al) (cycle no. 17 as a cyclic steady state) at 318 K and 4.5 bar.

Figure 9. As shown in Figure 9a,b, the cycle starts with pressurization with pure N_2, afterward, the adsorption step is started, followed by the rinse step with pure CO_2, to get the highest possible CO_2 concentration during the blowdown step. On these grounds, the CO_2 molar fraction increases during the blowdown and reduces through the purge step accompanied by a reverse orientation for N_2, as clarified in Figure 9a,b. Finally, by getting an almost regenerated bed with N_2 during the purge under a vacuum (0.2 bar), the column is prepared for the next cycle. Routinely, the yield of the cyclic adsorption process is evaluated regarding the purity, recovery, productivity, and energy consumption of the process (by eqs 1−6), for which these calculated factors for CO_2 and N_2 are illustrated in Figure 10. As can be observed, the designed VPSA demonstrates a capacity for getting CO_2 and N_2 with a purity of 67.3 and 99.3%, respectively. On the other hand, around 99.1 and 81% of CO_2 and N_2 can be recovered throughout the process. As the pressurization, adsorption, and rinse steps require a compressor as well as the blowdown and purge steps require a vacuum pump, the energy consumption of the process increases when compared to the ones that do not use vacuum pumps for regeneration steps. Besides the higher and lower pressure levels required by the pumps, another factor that can influence the energy consumption is the time of the process steps. In regeneration steps, for instance, increasing step times results in an increase of the energy consumption.

https://doi.org/10.1021/acs.iecr.4c00611
Ind. Eng. Chem. Res. 2024, 63, 8772−8785

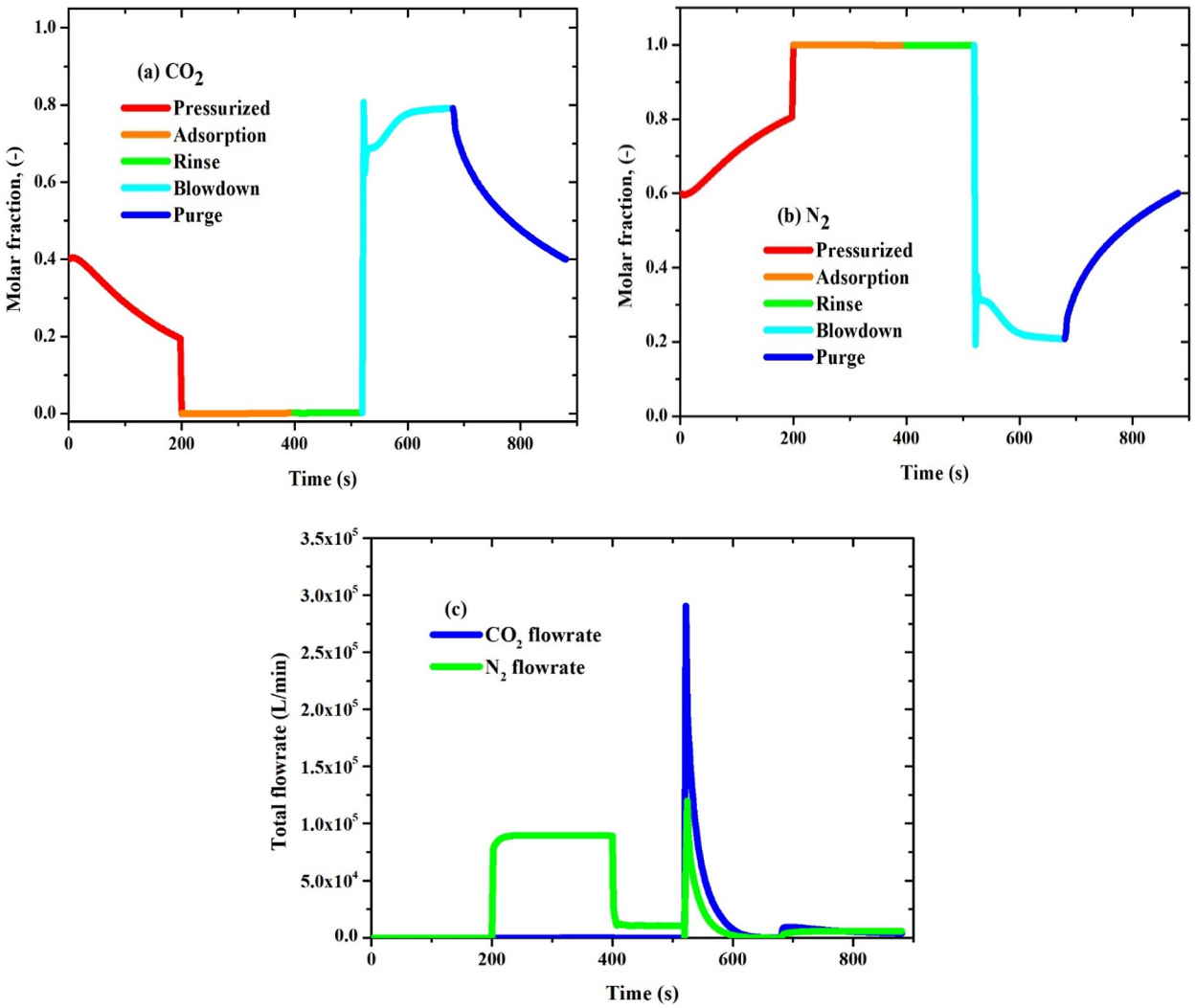

Figure 9. (a) Molar fraction of carbon dioxide, (b) molar fraction of nitrogen, and (c) flow rates of the designed industrial PSA process for CO_2 capture from flue gas using shaped MIL-160(Al) (cycle no. 17 as a cyclic steady state) at 318 K and 4.5 bar.

This process presented an energy consumption of 12.5 MW, as seen in Figure 10c.

To have a better grasp concerning the potential of shaped MIL-160(Al) for CO_2 capture for postcombustion application, a comparison with other reported benchmark adsorbents has been presented in Table S4 (Supporting Information). For instance, comparing MIL-160(Al) with zeolite 13X as one of the benchmark adsorbents for CO_2 capture, accomplished in a same condition (1-bed, 5-steps),[71] specified a better performance of MOF MIL-160(Al) for such purpose. Hence, regarding the remarkable specifications of MIL-160(Al) as a water stable MOF, which can capture CO_2 from flue gas under wet operating condition, synthesis in an easy sustainable way under ambient pressure conditions, the use of a bioderived ligand (2,5-FDCA or 2,5-furane dicarboxylic acid) with a rational synthesis cost accompanied by its stability and being in the shaped form,[50,51,55] as well as the acceptable CO_2/N_2 selectivity with the moderate heat of adsorption of CO_2 and N_2 (around −28.5 and −7.2 kJ/mol, respectively),[49] nominate MIL-160(Al) as an appealing adsorbent for carbon capture in industrial applications in comparison with benchmark ones (see Table S4).

5. CONCLUSIONS

In the way of accomplished efforts for carbon capture and climate change mitigation, in this study, the capacity of shaped MIL-160(Al) for separation of CO_2/N_2 concerning the postcombustion application was investigated. Accordingly, first the dynamic equilibrium adsorption of CO_2 and N_2 at 318 K and 4 bar was experimentally measured. Afterward, the dynamic outcomes were modeled using the developed equations and auxiliary relations. However, there were an acceptable agreement among the simulation and experimental results, which also proved the potential of considered model for designing a cyclic adsorption process. Next, relying on dynamic consequences, a PSA process with five steps was developed and experimentally validated for separation of the CO_2/N_2 mixture using a laboratory-scale setup. Finally, the large-scale capacity of MIL-160(Al) for postcombustion application was evaluated in the VPSA designed. The results showed the purity of CO_2 and N_2 around 67.3 and 99.3%, respectively, and the recovery around 99.1 and 81.1%, respectively. The arising results from this work accompanied by superb textural characteristics and specifications of MIL-160(Al) demonstrate a privileged potential of this adsorbent for carbon capture from flue gas. However, as future research

https://doi.org/10.1021/acs.iecr.4c00611
Ind. Eng. Chem. Res. 2024, 63, 8772−8785

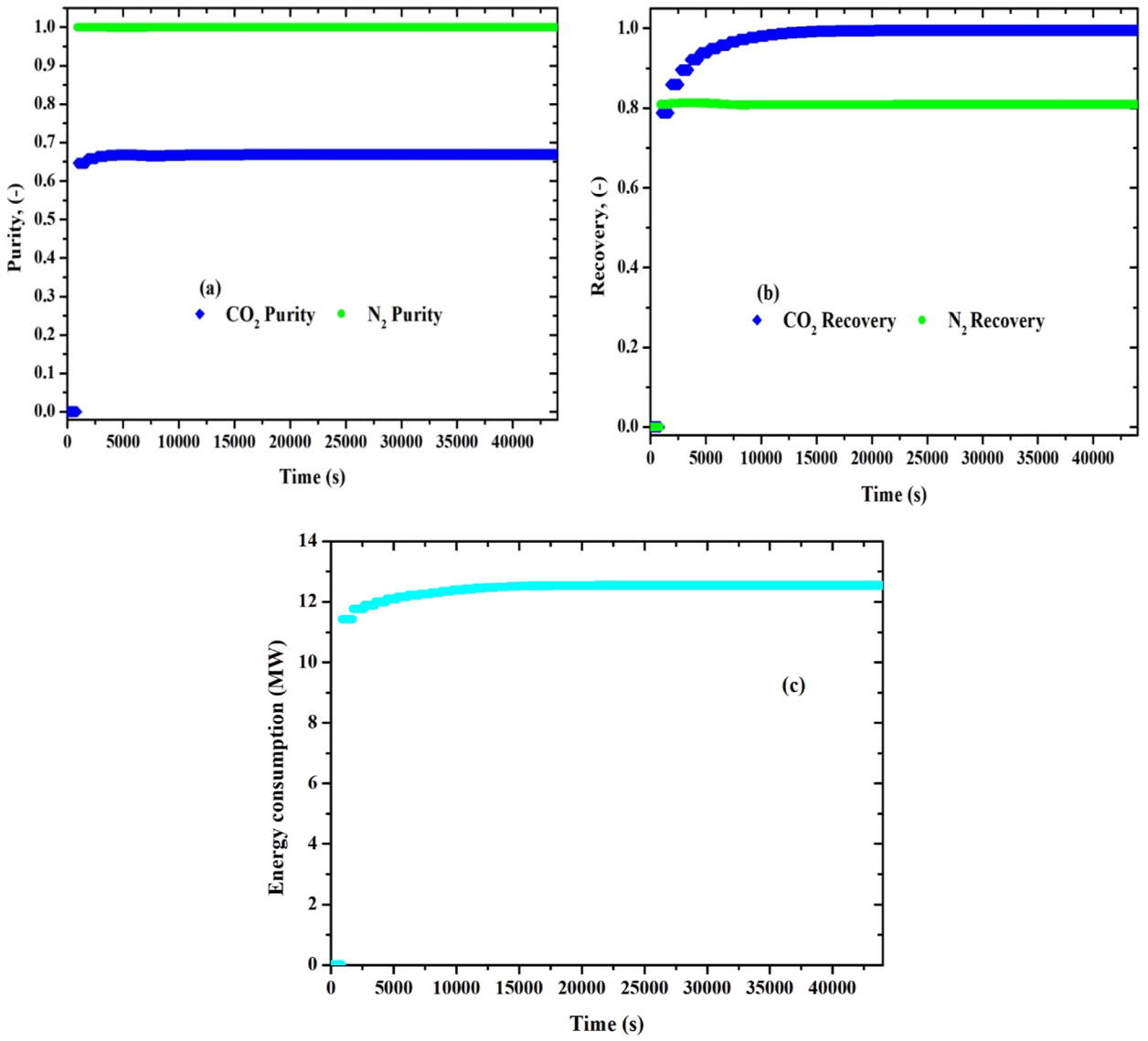

Figure 10. (a) Purity and (b) recovery of carbon dioxide and nitrogen, accompanied by (c) energy consumption of designed industrial PSA process for CO_2 capture from flue gas throughout all process (50 cycles).

directions, the study of MIL-160(Al) under the wet operating condition in the $CO_2/N_2/H_2O$ mixture by developing dynamic breakthrough experiments and cyclic adsorption process, as well as its comparison with other recently disclosed Al MOF MIL-120, that is very cheap and highly stable,[72] are suggested to be taken into account.

■ ASSOCIATED CONTENT

Supporting Information

The Supporting Information is available free of charge at https://pubs.acs.org/doi/10.1021/acs.iecr.4c00611.

N_2 adsorption−desorption isotherm at 77 K; detailed description of the developed model; full cycles of accomplished PSA experiment in the laboratory setup; CSS cycles of the designed industrial PSA process; and comparing some of the recent studied adsorbents for CO_2 capture from flue gas by the (V)PSA process (PDF)

■ AUTHOR INFORMATION

Corresponding Author

Mohsen Karimi − *Laboratory of Separation and Reaction Engineering (LSRE), Associate Laboratory LSRE/LCM, Faculty of Engineering and ALiCE—Associate Laboratory in Chemical Engineering, Faculty of Engineering, University of Porto, 4200-465 Porto, Portugal;* orcid.org/0000-0002-1886-5454; Phone: +351 934 070 714; Email: mohsen.karimi@fe.up.pt

Authors

Rafael M. Siqueira − *Laboratory of Separation and Reaction Engineering (LSRE), Associate Laboratory LSRE/LCM, Faculty of Engineering and ALiCE—Associate Laboratory in Chemical Engineering, Faculty of Engineering, University of Porto, 4200-465 Porto, Portugal*

Alírio E. Rodrigues − *Laboratory of Separation and Reaction Engineering (LSRE), Associate Laboratory LSRE/LCM, Faculty of Engineering and ALiCE—Associate Laboratory in Chemical Engineering, Faculty of Engineering, University of*

https://doi.org/10.1021/acs.iecr.4c00611
Ind. Eng. Chem. Res. 2024, 63, 8772−8785

Porto, 4200-465 Porto, Portugal; orcid.org/0000-0002-0715-4761

Farid Nouar − *Institut des Matériaux Poreux de Paris, ESPCI Paris, Ecole Normale Supérieure, CNRS, PSL University, 75005 Paris, France*

José A. C. Silva − *Centro de Investigação de Montanha (CIMO), Instituto Politécnico de Bragança, 5300-253 Bragança, Portugal; Laboratório Associado para a Sustentabilidade e Tecnologia em Regiões de Montanha (SusTEC), Instituto Politécnico de Bragança, 5300-253 Bragança, Portugal;* orcid.org/0000-0003-1778-3833

Christian Serre − *Institut des Matériaux Poreux de Paris, ESPCI Paris, Ecole Normale Supérieure, CNRS, PSL University, 75005 Paris, France;* orcid.org/0000-0003-3040-2564

Alexandre F. P. Ferreira − *Laboratory of Separation and Reaction Engineering (LSRE), Associate Laboratory LSRE/LCM, Faculty of Engineering and ALiCE—Associate Laboratory in Chemical Engineering, Faculty of Engineering, University of Porto, 4200-465 Porto, Portugal;* orcid.org/0000-0002-6746-8973

Complete contact information is available at: https://pubs.acs.org/10.1021/acs.iecr.4c00611

Notes

The authors declare no competing financial interest.

■ ACKNOWLEDGMENTS

This work was financially supported by LA/P/0045/2020 (ALiCE), UIDB/50020/2020, and UIDP/50020/2020 (LSRE-LCM), funded by national funds through FCT/MCTES (PIDDAC). It also received financial support by national funds through FCT/MCTES (PIDDAC): CIMO, UIDB/00690/2020 (DOI: 10.54499/UIDB/00690/2020) and UIDP/00690/2020 (DOI: 10.54499/UIDP/00690/2020), and SusTEC, LA/P/0007/2020 (DOI: 10.54499/LA/P/0007/2020). The authors also acknowledge Kyung-Ho Cho and U-Hwang Lee from the Korea Research Institute of Chemical Technology (KRICT), Republic of Korea, for their contributions in the shaping MIL-160(Al). M.K. acknowledges research grants awarded by the Foundation of Science and Technology of Portugal (FCT) under SFRH/BD/140550/2018 project and the University of Porto under FEUP-BioGasUpGMIL160 project.

■ REFERENCES

(1) Karimi, M.; C Silva, J. A.; Gonçalves, C. N. d. P.; L Diaz de Tuesta, J.; Rodrigues, A. E.; Gomes, H. T. CO2 Capture in Chemically and Thermally Modified Activated Carbons Using Breakthrough Measurements: Experimental and Modeling Study. *Ind. Eng. Chem. Res.* **2018**, *57* (32), 11154−11166.

(2) Akeeb, O.; Wang, L.; Xie, W.; Davis, R.; Alkasrawi, M.; Toan, S. Post-Combustion CO2 Capture via a Variety of Temperature Ranges and Material Adsorption Process: A Review. *J. Environ. Manage.* **2022**, *313*, 115026.

(3) Henrique, A.; Karimi, M.; Silva, J. A. C.; Rodrigues, A. E. Analyses of Adsorption Behavior of CO 2, CH 4, and N 2 on Different Types of BETA Zeolites. *Chem. Eng. Technol.* **2019**, *42* (2), 327−342.

(4) Raganati, F.; Miccio, F.; Ammendola, P. Adsorption of Carbon Dioxide for Post-Combustion Capture: A Review. *Energy Fuels* **2021**, *35* (16), 12845−12868.

(5) Samanta, A.; Zhao, A.; Shimizu, G. K. H.; Sarkar, P.; Gupta, R. Post-Combustion CO2 Capture Using Solid Sorbents: A Review. *Ind. Eng. Chem. Res.* **2012**, *51* (4), 1438−1463.

(6) GISTEMP Team. GISS Surface Temperature Analysis (GISTEMP), Version 4. NASA Goddard Institute for Space Studies. 2022, https://data.giss.nasa.gov/gistemp/ (accessed Nov 02, 2022).

(7) NASA-GISS. Goddard Institute for Space Studies. 2022, https://data.giss.nasa.gov/gistemp/ (accessed Nov 02, 2022).

(8) Earth Now—Climate Change: Vital Signs of the Planet. https://climate.nasa.gov/earth-now/ (accessed April 01, 2024).

(9) Shirzad, M.; Karimi, M.; Rodrigues, A. E.; Silva, J. A. C. Biochar in Carbon Sequestration. In *Biochar and its Composites: Fundamentals and Applications*, 1st ed.; Springer Nature, 2023; Vol. Part *F1442*, pp 73−105.

(10) Shahhoseini, E.; Arefifard, M.; Karimi, M. Biochar for Climate Change Mitigation. In *Biochar and its Composites: Fundamentals and Applications*, 1st ed.; Springer Nature, 2023; Vol. Part *F1442*, pp 123−143.

(11) Arias, P.; Bellouin, N.; Coppola, E.; Jones, R.; Krinner, G.; Marotzke, J.; Naik, V.; Palmer, M.; Plattner, G.-K.; Rogelj, J.; et al. Climate Change 2021: The Physical Science Basis. Contribution of Working Group14 I to the Sixth Assessment Report of the Intergovernmental Panel on Climate Change; Technical Summary, Cambridge. 2021, https://www.ipcc.ch/report/ar6/wg1/ (accessed Nov 18, 2021).

(12) Chen, X.; Wang, J.; Du, T.; Liu, L.; Wang, Y.; Kevin Li, G. Post-Combustion CO2 Capture Using Exchanger Type Vacuum Temperature Swing Adsorption: Cycle Design and Performance Analysis. *Energy Convers. Manag.* **2023**, *296*, 117625.

(13) Daryayehsalameh, B.; Nabavi, M.; Vaferi, B. Modeling of CO2 Capture Ability of [Bmim] [BF4] Ionic Liquid Using Connectionist Smart Paradigms. *Environ. Technol. Innov* **2021**, *22*, 101484.

(14) Karimi, M.; Diaz de Tuesta, J. L.; d P Gonçalves, C. N.; Gomes, H. T.; Rodrigues, A. E.; Silva, J. A. C. Compost from Municipal Solid Wastes as a Source of Biochar for CO2 Capture. *Chem. Eng. Technol.* **2020**, *43* (7), 1336−1349.

(15) Karimi, M.; Rodrigues, A. E.; Silva, J. A. C. Designing a Simple Volumetric Apparatus for Measuring Gas Adsorption Equilibria and Kinetics of Sorption. Application and Validation for CO2, CH4 and N2 Adsorption in Binder-Free Beads of 4A Zeolite. *Chem. Eng. J.* **2021**, *425*, 130538.

(16) Karimi, M.; Rodrigues, A. E.; Silva, J. A. C. Biomass as a Source of Adsorbents for CO2 Capture. In *Advances in Bioenergy and Microfluidic Applications*, 1st ed.; Elsevier: Amsterdam, 2021; pp 255−274.

(17) Webley, P. A. Adsorption Technology for CO2 Separation and Capture: A Perspective. *Adsorption* **2014**, *20* (2−3), 225−231.

(18) Bui, M.; Adjiman, C. S.; Bardow, A.; Anthony, E. J.; Boston, A.; Brown, S.; Fennell, P. S.; Fuss, S.; Galindo, A.; Hackett, L. A.; Hallett, J. P.; Herzog, H. J.; Jackson, G.; Kemper, J.; Krevor, S.; Maitland, G. C.; Matuszewski, M.; Metcalfe, I. S.; Petit, C.; Puxty, G.; Reimer, J.; Reiner, D. M.; Rubin, E. S.; Scott, S. A.; Shah, N.; Smit, B.; Trusler, J. P. M.; Webley, P.; Wilcox, J.; mac Dowell, N. Carbon Capture and Storage (CCS): The Way Forward. *Energy Environ. Sci.* **2018**, *11* (5), 1062−1176.

(19) Zhou, Z.; Davoudi, E.; Vaferi, B. Monitoring the Effect of Surface Functionalization on the CO2 Capture by Graphene Oxide/Methyl Diethanolamine Nanofluids. *J. Environ. Chem. Eng.* **2021**, *9* (5), 106202.

(20) Karimi, M.; Shirzad, M.; Silva, J. A. C.; Rodrigues, A. E. Carbon Dioxide Separation and Capture by Adsorption: A Review. *Environ. Chem. Lett.* **2023**, *21*, 2041−2084.

(21) Ben-Mansour, R.; Habib, M. A.; Bamidele, O. E.; Basha, M.; Qasem, N. A. A.; Peedikakkal, A.; Laoui, T.; Ali, M. Carbon Capture by Physical Adsorption: Materials, Experimental Investigations and Numerical Modeling and Simulations - A Review. *Appl. Energy* **2016**, *161*, 225−255.

(22) Liu, R. S.; Shi, X. D.; Wang, C. T.; Gao, Y. Z.; Xu, S.; Hao, G. P.; Chen, S.; Lu, A. H. Advances in Post-Combustion CO2 Capture

by Physical Adsorption: From Materials Innovation to Separation Practice. *ChemSusChem* **2021**, *14* (6), 1428−1471.
(23) Dhoke, C.; Zaabout, A.; Cloete, S.; Amini, S. Review on Reactor Configurations for Adsorption-Based CO2 Capture. *Ind. Eng. Chem. Res.* **2021**, *60* (10), 3779−3798.
(24) Karimi, M.; Shirzad, M.; Silva, J. A. C.; Rodrigues, A. E. Biomass/Biochar Carbon Materials for CO2 Capture and Sequestration by Cyclic Adsorption Processes: A Review and Prospects for Future Directions. *J. CO_2 Util.* **2022**, *57*, 101890.
(25) Canevesi, R.; Andreassen, K.; da Silva, E. A.; Borba, C.; Grande, C. Pressure Swing Adsorption for Biogas Upgrading with Carbon Molecular Sieve. *Ind. Eng. Chem. Res.* **2018**, *57* (23), 8057−8067.
(26) Rocha, L. A. M.; Andreassen, K. A.; Grande, C. A. Separation of CO2/CH4 Using Carbon Molecular Sieve (CMS) at Low and High Pressure. *Chem. Eng. Sci.* **2017**, *164*, 148−157.
(27) Joss, L.; Gazzani, M.; Mazzotti, M. Rational Design of Temperature Swing Adsorption Cycles for Post-Combustion CO2 Capture. *Chem. Eng. Sci.* **2017**, *158*, 381−394.
(28) Marx, D.; Joss, L.; Hefti, M.; Mazzotti, M. Temperature Swing Adsorption for Postcombustion CO2 Capture: Single- and Multicolumn Experiments and Simulations. *Ind. Eng. Chem. Res.* **2016**, *55* (5), 1401−1412.
(29) Zafanelli, L. F. A. S.; Henrique, A.; Karimi, M.; Rodrigues, A. E.; Silva, J. A. C. Single- A Nd Multicomponent Fixed Bed Adsorption of CO2, CH4, and N2in Binder-Free Beads of 4A Zeolite. *Ind. Eng. Chem. Res.* **2020**, *59* (30), 13724−13734.
(30) Karimi, M.; Zafanelli, L. F. A. S.; Almeida, J. P. P.; Ströher, G. R.; Rodrigues, A. E.; Silva, J. A. C. Novel Insights into Activated Carbon Derived from Municipal Solid Waste for CO2 Uptake: Synthesis, Adsorption Isotherms and Scale-Up. *J. Environ. Chem. Eng.* **2020**, *8* (5), 104069.
(31) Durán, I.; Álvarez-Gutiérrez, N.; Rubiera, F.; Pevida, C. Biogas Purification by Means of Adsorption on Pine Sawdust-Based Activated Carbon: Impact of Water Vapor. *Chem. Eng. J.* **2018**, *353*, 197−207.
(32) Ryckebosch, E.; Drouillon, M.; Vervaeren, H. Techniques for Transformation of Biogas to Biomethane. *Biomass Bioenergy* **2011**, *35* (5), 1633−1645.
(33) Ferreira, A. F. P.; Ribeiro, A. M.; Kulaç, S.; Rodrigues, A. E. Methane Purification by Adsorptive Processes on MIL-53(Al). *Chem. Eng. Sci.* **2015**, *124*, 79−95.
(34) Keskin, S.; van Heest, T.; Sholl, D. S. Can Metal-Organic Framework Materials Play a Useful Role in Large-Scale Carbon Dioxide Separations? *ChemSusChem* **2010**, *3* (8), 879−891.
(35) Ding, M.; Flaig, R. W.; Jiang, H. L.; Yaghi, O. M. Carbon Capture and Conversion Using Metal-Organic Frameworks and MOF-Based Materials. *Chem. Soc. Rev.* **2019**, *48* (10), 2783−2828.
(36) Dai, S.; Tissot, A.; Serre, C. Recent Progresses in Metal-Organic Frameworks Based Core-Shell Composites. *Adv. Energy Mater.* **2022**, *12* (4), 2100061.
(37) Nikolaidis, G. N.; Kikkinides, E. S.; Georgiadis, M. C. An Integrated Two-Stage P/VSA Process for Postcombustion CO2 Capture Using Combinations of Adsorbents Zeolite 13X and Mg-MOF-74. *Ind. Eng. Chem. Res.* **2017**, *56* (4), 974−988.
(38) Ye, S.; Jiang, X.; Ruan, L. W.; Liu, B.; Wang, Y. M.; Zhu, J. F.; Qiu, L. G. Post-Combustion CO2 Capture with the HKUST-1 and MIL-101(Cr) Metal-Organic Frameworks: Adsorption, Separation and Regeneration Investigations. *Microporous Mesoporous Mater.* **2013**, *179*, 191−197.
(39) Sabri, N. H.; Rani, N. H. A.; Mohamad, N. F.; Mohd Muhsen, N. A. S.; Md Zaini, M. S. Simulation of CO2 Capture for Amine Impregnated Activated Carbon - Palm Kernel Shell (AC-PKS) Adsorbent in Pressure Swing Adsorption (PSA) Using Aspen Adsorption. *Mater. Today Proc.* **2023**, DOI: 10.1016/j.matpr.2022.12.206.
(40) Raganati, F.; Chirone, R.; Ammendola, P. CO2 Capture by Temperature Swing Adsorption: Working Capacity As Affected by Temperature and CO2 Partial Pressure. *Ind. Eng. Chem. Res.* **2020**, *59* (8), 3593−3605.
(41) Dantas, T. L. P.; Luna, F. M. T.; Silva, I. J.; Torres, A. E. B.; de Azevedo, D. C. S.; Rodrigues, A. E.; Moreira, R. F. P. M. Carbon Dioxide-Nitrogen Separation through Pressure Swing Adsorption. *Chem. Eng. J.* **2011**, *172* (2−3), 698−704.
(42) Kacem, M.; Pellerano, M.; Delebarre, A. Pressure Swing Adsorption for CO2/N2 and CO2/CH4 Separation: Comparison between Activated Carbons and Zeolites Performances. *Fuel Process. Technol.* **2015**, *138*, 271−283.
(43) Mendes, P. A. P.; Ribeiro, A. M.; Gleichmann, K.; Ferreira, A. F. P.; Rodrigues, A. E. Separation of CO2/N2 on Binderless 5A Zeolite. *J. CO_2 Util.* **2017**, *20*, 224−233.
(44) Ben-Mansour, R.; Bamidele, O. E.; Habib, M. A. Evaluation of Mg-MOF-74 for Post-Combustion Carbon Dioxide Capture through Pressure Swing Adsorption. *Int. J. Energy Res.* **2015**, *39* (15), 1994−2007.
(45) Pirngruber, G. D.; Leinekugel-Le-Cocq, D. Design of a Pressure Swing Adsorption Process for Postcombustion CO 2 Capture. *Ind. Eng. Chem. Res.* **2013**, *52* (17), 5985−5996.
(46) Nguyen, T. T. T.; Lin, J. B.; Shimizu, G. K. H.; Rajendran, A. Separation of CO2 and N2 on a Hydrophobic Metal Organic Framework CALF-20. *Chem. Eng. J.* **2022**, *442*, 136263.
(47) Maurin, G.; Serre, C.; Cooper, A.; Férey, G. The New Age of MOFs and of Their Porous-Related Solids. *Chem. Soc. Rev.* **2017**, *46* (11), 3104−3107.
(48) Mahajan, S.; Lahtinen, M. Recent Progress in Metal-Organic Frameworks (MOFs) for CO2 Capture at Different Pressures. *J. Environ. Chem. Eng.* **2022**, *10* (6), 108930.
(49) Karimi, M.; Ferreira, A.; Rodrigues, A. E.; Nouar, F.; Serre, C.; Silva, J. A. C. MIL-160(Al) as a Candidate for Biogas Upgrading and CO2 Capture by Adsorption Processes. *Ind. Eng. Chem. Res.* **2023**, *62* (12), 5216−5229.
(50) Permyakova, A.; Skrylnyk, O.; Courbon, E.; Affram, M.; Wang, S.; Lee, U. H.; Valekar, A. H.; Nouar, F.; Mouchaham, G.; Devic, T.; De Weireld, G.; Chang, J. S.; Steunou, N.; Frère, M.; Serre, C. Synthesis Optimization, Shaping, and Heat Reallocation Evaluation of the Hydrophilic Metal-Organic Framework MIL-160(Al). *ChemSusChem* **2017**, *10* (7), 1419−1426.
(51) Cadiau, A.; Lee, J. S.; Damasceno Borges, D.; Fabry, P.; Devic, T.; Wharmby, M. T.; Martineau, C.; Foucher, D.; Taulelle, F.; Jun, C.-H.; Hwang, Y. K.; Stock, N.; de Lange, M. F.; Kapteijn, F.; Gascon, J.; Maurin, G.; Chang, J.-S.; Serre, C.; Cadiau, A.; Fabry, P.; Devic, T.; Martineau, C.; Foucher, D.; Taulelle, F.; Serre, C.; Lee, J. S.; Hwang, Y. K.; Chang, J.-S.; Jun, C.-H.; Damasceno-Borges, D.; Maurin, G.; de Lange, M. F.; Kapteijn, F.; Gascon, J. Design of Hydrophilic Metal Organic Framework Water Adsorbents for Heat Reallocation. *Adv. Mater.* **2015**, *27* (32), 4775−4780.
(52) Damasceno Borges, D.; Maurin, G.; Galvão, D. S. Design of Porous Metal-Organic Frameworks for Adsorption Driven Thermal Batteries. *MRS Adv.* **2017**, *2* (9), 519−524.
(53) Mouchaham, G.; Cui, F. S.; Nouar, F.; Pimenta, V.; Chang, J. S.; Serre, C. Metal-Organic Frameworks and Water: 'From Old Enemies to Friends'? *Trends Chem.* **2020**, *2* (11), 990−1003.
(54) Chakraborty, D.; Yurdusen, A.; Mouchaham, G.; Nouar, F.; Serre, C. Large-Scale Production of Metal-Organic Frameworks. *Adv. Funct. Mater.* **2023**, 2309089.
(55) Severino, M. I.; Gkaniatsou, E.; Nouar, F.; Pinto, M. L.; Serre, C. MOFs Industrialization: A Complete Assessment of Production Costs. *Faraday Discuss.* **2021**, *231* (0), 326−341.
(56) Karimi, M. Process Development for Carbon Dioxide Capture Using Novel Adsorbents: Applications for Clean Energy and Environmental Protection. Ph.D. Dissertation, University of Porto, Porto, 2023.
(57) Foo, K. Y.; Hameed, B. H. Insights into the Modeling of Adsorption Isotherm Systems. *Chem. Eng. J.* **2010**, *156* (1), 2−10.
(58) Langmuir, I. The Constitution and Fundamental Properties of Solids and Liquids. Part I. Solids. *J. Am. Chem. Soc.* **1916**, *38* (11), 2221−2295.

(59) Do, D. D. *Adsorption Analysis: Equilibria and Kinetics (With CD Containing Computer Matlab Programs)*, 1st ed.; Series on Chemical Engineering; Imperial College Press: London, 1998; Vol. 2.
(60) Ruthven, D. M. *Principles of Adsorption and Adsorption Processes*, 1st ed.; Wiley: New York, 1984.
(61) Pérez-Marín, A. B.; Zapata, V. M.; Ortuño, J.; Aguilar, M.; Sáez, J.; Lloréns, M. Removal of Cadmium from Aqueous Solutions by Adsorption onto Orange Waste. *J. Hazard. Mater.* **2007**, *139* (1), 122−131.
(62) Vijayaraghavan, K.; Padmesh, T. V. N.; Palanivelu, K.; Velan, M. Biosorption of Nickel(II) Ions onto Sargassum Wightii: Application of Two-Parameter and Three-Parameter Isotherm Models. *J. Hazard. Mater.* **2006**, *133* (1−3), 304−308.
(63) Kundu, S.; Gupta, A. K. Arsenic Adsorption onto Iron Oxide-Coated Cement (IOCC): Regression Analysis of Equilibrium Data with Several Isotherm Models and Their Optimization. *Chem. Eng. J.* **2006**, *122* (1−2), 93−106.
(64) Rao, M. B.; Sircar, S. Thermodynamic Consistency for Binary Gas Adsorption Equilibria. *Langmuir* **1999**, *15* (21), 7258−7267.
(65) Karimi, M.; Rahimpour, M. R.; Rafiei, R.; Shariati, A.; Iranshahi, D. Improving Thermal Efficiency and Increasing Production Rate in the Double Moving Beds Thermally Coupled Reactors by Using Differential Evolution (DE) Technique. *Appl. Therm. Eng.* **2016**, *94*, 543−558.
(66) Karimi, M.; Rahimpour, M. R.; Iranshahi, D. Enhanced BTX Production in Refineries with Sulfur Dioxide Oxidation by Thermal Integrated Model. *Chem. Eng. Technol.* **2018**, *41* (9), 1746−1758.
(67) Karimi, M.; Siqueira, R. M.; Rodrigues, A. E.; Nouar, F.; Silva, J. A. C.; Serre, C.; Ferreira, A. Biogas Upgrading Using Shaped MOF MIL-160(Al) by Pressure Swing Adsorption Process: Experimental and Dynamic Modelling Assessment. *Sep. Purif. Technol.* **2024**, *344*, 127260.
(68) Rota, R.; Wankat, P. C. Intensification of Pressure Swing Adsorption Processes. *AIChE J.* **1990**, *36* (9), 1299−1312.
(69) Ribeiro, A. M.; Santos, J. C.; Rodrigues, A. E. Pressure Swing Adsorption for CO2 Capture in Fischer−Tropsch Fuels Production from Biomass. *Adsorption* **2011**, *17* (3), 443−452.
(70) Agarwal, A.; Biegler, L. T.; Zitney, S. E. A Superstructure-Based Optimal Synthesis of PSA Cycles for Post-Combustion CO2 Capture. *AIChE J.* **2010**, *56* (7), 1813−1828.
(71) Park, J. H.; Beum, H. T.; Kim, J. N.; Cho, S. H. Numerical Analysis on the Power Consumption of the PSA Process for Recovering CO2 from Flue Gas. *Ind. Eng. Chem. Res.* **2002**, *41* (16), 4122−4131.
(72) Chen, B.; Fan, D.; Pinto, R. V.; Dovgaliuk, I.; Nandi, S.; Chakraborty, D.; García-Moncada, N.; Vimont, A.; McMonagle, C. J.; Bordonhos, M.; Al Mohtar, A.; Cornu, I.; Florian, P.; Heymans, N.; Daturi, M.; De Weireld, G.; Pinto, M.; Nouar, F.; Maurin, G.; Mouchaham, G.; Serre, C. A Scalable Robust Microporous Al-MOF for Post-Combustion Carbon Capture. *Adv. Sci.* **2024**, 2401070.

https://doi.org/10.1021/acs.iecr.4c00611
Ind. Eng. Chem. Res. 2024, 63, 8772−8785